

CLASSIFICATION AND MULTIVARIATE ANALYSIS
OF DIFFERENCES IN GROSS PRIMARY
PRODUCTION AT DIFFERENT ELEVATIONS
USING BIOME-BGC IN THE PÁRAMOS,
ECUADORIAN ANDEAN REGION

CLASIFICACIÓN Y ANÁLISIS MULTIVARIADO DE
DIFERENCIAS EN PRODUCCIÓN PRIMARIA
BRUTA EN DIFERENTES ELEVACIONES USANDO
BIOME-BGC EN LOS PÁRAMOS, REGIÓN ANDINA
ECUATORIANA

VERONICA MINAYA* GERALD CORZO[†]
JOHANNES VAN DER KWAST[‡] REMIGIO GALÁRRAGA[§]
ARTHUR MYNETT[¶]

*Received: 24/Feb/2014; Revised: 6/Mar/2015;
Accepted: 20/May/2015*

Abstract

Gross primary production (GPP) in climate change studies with multi-species and elevation variables are difficult to measure and simulate. Models tend to provide a representation of dynamic process through long-term analysis by using generalized parameterizations. Even, current approaches of modelling do not contemplate easily the variation of GPP at different elevations for different vegetation types in regions like *páramos*, mainly due to data unavailability. In these models information from cells is commonly averaged, and therefore average elevation, ecophysiology of vegetation, as well as other parameters is generalized. The vegetation model BIOME-BGC was applied to the Ecuadorian Andean region for elevations greater than 4000 masl with the presence of typical vegetation of *páramo* for 10 years of simulation (period 2000-2009). An estimation of the difference of GPP obtained using a generalized altitude and predominant type of vegetation could lead to a better estimation of the uncertainty in the magnitude of the errors in global climate models. This research explores GPP from 3 different altitudes and 3 vegetation types against 2 main climate drivers (Short Wave Radiation and Vapor Pressure Deficit). Since it is important to measure the possible errors or difference in the use of averaged meteorological and ecophysiological data, here we present a multivariate analysis of the dynamic difference of GPP in time, relative to an altitude and type of vegetation. A copula multivariable model allows us to identify and classify the changes in GPP per type of vegetation and altitude. The Frank copula model of joint distributions was our best fit between GPP and climate drivers and it allowed us to understand better the dependency of the variables. These results can explore extreme situations where averaged simplified approaches could mislead. The change of GPP over time is essential for future climate scenarios of the ecosystem storage and release of carbon to the atmosphere. Our findings suggest that a classification of the difference is highly important to be extended to cells that have similar properties.

Keywords: multivariate classification; copula; BIOME-BGC; GPP; *páramos*.

*UNESCO-IHE, Institute for Water Education, Delft, The Netherlands; & . E-Mail: v.minayamaldonado@unesco-ihe.org

†UNESCO-IHE, Institute for Water Education, Delft, The Netherlands. E-Mail: g.corzo@unesco-ihe.org

‡Misma dirección que/Same address as: G. Corzo. E-Mail: h.vanderkwast@unesco-ihe.org

§Escuela Politécnica Nacional, Quito, Ecuador. E-Mail: remigala@mail.epn.edu.ec, remigala@hotmail.com

¶UNESCO-IHE, Institute for Water Education & Technological University of Delft, TU-Delft, Delft, The Netherlands. E-Mail: a.mynett@unesco-ihe.org

Resumen

La producción primaria (GPP) es difícil de medir y simular en estudios de cambio climático con múltiples especies de vegetación y con variabilidad en elevación. Los modelos tienden a proveer una representación de los procesos dinámicos a través de análisis a largo plazo usando parametrizaciones generalizadas. Incluso métodos actualizados de modelación no contemplan fácilmente la variación de GPP a diferentes elevaciones y para diferentes tipos de vegetación en regiones como los *páramos*, debido principalmente a la inexistencia de datos. En estos modelos, la información de las celdas son comúnmente promediadas y por lo tanto factores como la elevación media, eco-fisiología de la vegetación y otros parámetros son generalizados. El modelo de vegetación BIOME-BGC fue aplicado en un área de estudio dentro de la región andina Ecuatoriana a elevaciones superiores a los 4000 msnm donde existe una presencia típica de vegetación de *páramo* para 10 años de simulación (periodo 2000-2009). La estimación de la diferencia de la GPP obtenida usando una generalización de altura y tipo de vegetación predominante puede conducir a una mejor estimación de la incertidumbre en la magnitud de los errores en modelos climáticos globales. Este estudio explora la relación entre la GPP de tres tipos de vegetación agrupados de acuerdo a sus formas de crecimiento a tres rangos altitudinales y dos factores climáticos (Radiación de onda corta y deficiencia de presión de vapor). Debido a la importancia de la medición de posibles errores o las diferencias en el uso de valores promedio de datos meteorológicos e ecofisiológicos, aquí presentamos un análisis multivariado de la diferencia dinámica de la GPP en el tiempo con respecto al rango altitudinal y al tipo de vegetación. El modelo multivariable Copula nos permite identificar y clasificar los cambios de GPP por tipo de vegetación y por rango altitudinal. El modelo cópula distribuido Frank fue el que mejor se acopló entre la GPP y las variables climáticas y nos permitió entender mejor la dependencia entre estas variables. Los resultados podrían explorar situaciones extremas donde estrategias simplificadas promedio podrían confundir. El cambio de GPP en el tiempo es esencial para futuros escenarios climáticos del almacenamiento y liberación de carbón del ecosistema hacia la atmósfera. Nuestros resultados sugieren que la clasificación de esta diferencia es muy importante que sea extendida a celdas que tienen propiedades similares.

Palabras clave: clasificación multivariada; cópula; BIOME-BGC; GPP; páramos.

Mathematics Subject Classification: 62H99.

1 Introduction

Many studies have demonstrated that an increased in atmospheric carbon dioxide (CO_2) in combination with global climate change might have serious consequences in the growth of terrestrial vegetation [40]. The Earth Observing System (EOS) of the U.S. National Aeronautics and Space Administration (NASA) is currently estimating the spatial variability of net primary production (NPP) and gross primary production (GPP) of the globe at 1-km spatial resolution for the last 14 years [29]. However, these estimations hardly contemplate the vegetation heterogeneity and the spatial variation of meteorological variables that are different within 1-km cell specifically for mountainous regions driven by microclimates. The estimates of GPP define more accurately the terrestrial CO_2 fluxes than the normalized difference vegetation indexes (NDVI) currently used [29]. The NPP and GPP products are of great value in our understanding on terrestrial and atmospheric carbon cycling dynamics.

Ecosystem terrestrial models deal with a certain degree of complexity not only to their inner processes but also to the amount of eco-physiological parameters needed to accurately reproduce the fluxes and states of water and nutrients of a defined biome [34, 31, 32, 42]. These models alone or in combination with satellite imagery have been successfully applied in the quantification of net primary production (NPP) and gross primary production (GPP) across the world at different spatial and temporal scales [20, 46, 16, 38]. These studies compare their simulations with measurements to evaluate the performance of the model and determine whether it is able to capture the dynamic process of the land carbon cycle. However, measurements are also susceptible to uncertainties due to the wide variety of measuring instruments, operator techniques, statistical analysis of a set of measurements [1] and the effects of variability and environmental heterogeneity characteristic of mountainous terrains [8]. For instance, the information required for tropical grasslands is not always readily accessible [9] and due to budget and time limitations measured values are usually averaged or generalized leading to a homogeneous parameterization that may distort the outcomes.

The use of mathematical tools that includes statistical probabilistic functions is widely applied to assess the spatial and temporal variability of environmental variables that are not linearly correlated in nature [6, 3]. In engineering, copulas are used in environmental space-time processes and hydrological modelling [45, 11]. The copula function constructs a required joint distribution that relates the dependence of random variables and their uniform marginals $[0,1]$ [10, 5, 13]. In this article we analyze the GPP changes due to climatic variations taking into account vegetation heterogeneity along an altitudinal gradient. This

will be compared to a GPP estimated on an averaged single measure to classify possible errors. Finally, the application of a Copula-based bivariate distribution will be used to assess undesirable extreme GPP production due to changes in climatic variables in the region.

2 Data sources

2.1 Study area

A typical region in the Ecuadorian Andes region was selected to be able to represent the Andean GPP changes. "Los Crespos - Humbolt" (LCH) basin was selected and it is located in the southwestern side of the volcano Antisana. It has an area of 15.2 km², of which 16% is covered by glacier, 17% by moraine and 68% with *páramo* vegetation and extends from 4010 masl to 5000 masl (Figure 1). This area is less than 1% in proportion to 50x50 km cell of most global climate models.

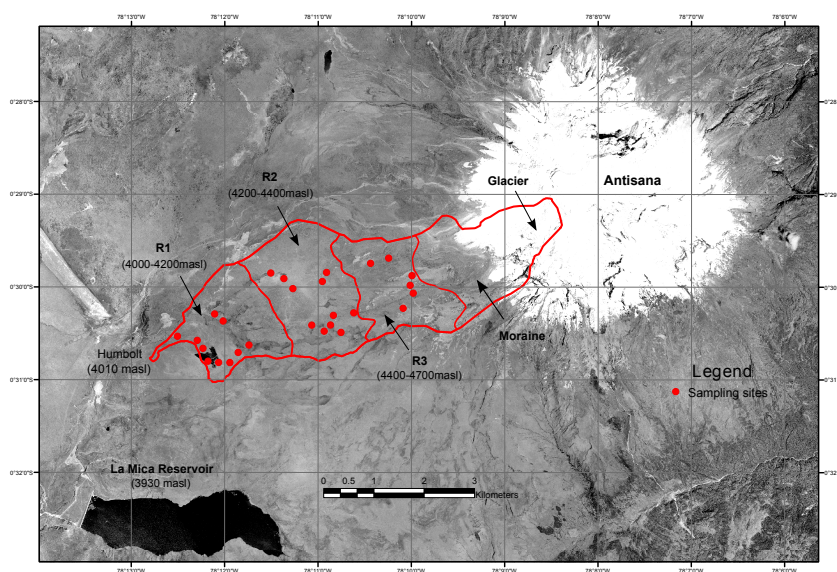


Figure 1: Location of the study sites in the "Los Crespos - Humbolt" Basin, Ecuador. (Source: ASTER Satellite Image, 15m resolution). A total of 27 sampling plots distributed in three altitudinal ranges from 4010 masl to 4700 masl.

Precipitation range is 800-1200 mm/yr, monthly average temperature is 6°C and average relative humidity is around 80%. Typical *páramo* vegetation covers the entire surface until the beginning of the moraine, which is mainly located at

elevations above 4700 masl. The main vegetation in the lower and mid catchment is dominated by tussock grasses (TU) (*Calamagrostis intermedia*) and acaulescent rosettes (AR) (*Werneria nubigena*, *Hypochaeris sessiliflora*). Near flood zones and streams there is a strong dominance of cushions (CU) (*Azorrella Pedunculata*) [22].

2.2 Meteorological data

Daily meteorological data were derived from IRD (Institut de recherche pour le développement - Ecuador) and INAMHI (Instituto Nacional de Meteorología e Hidrología en Ecuador) databases. Distinctively, daily total precipitation and daily maximum and minimum temperatures were collected from 2 stations, one located at 4000 masl (outlet of the basin) and the other at 4785 masl (upper basin) for the years 2000-2009 (Annex Table A1).

2.3 Plant ecophysiological parameters

From earlier vegetation inventories [22], we identified plant species that were classified based on their growth forms [28] with large differences in their carbon, nitrogen concentration and main ecophysiological characteristics. These parameters were adequately treated for each growth form (TU, AR, CU) at three different elevations (R1: 4000-4200 masl; R2: 4200-4400 masl; R3: 4400-4600 masl). Other additional information was derived from literature search and calculated mean and standard deviation (Annex Table A2).

2.4 Topographic and soil-related data

A Digital Terrain Model (DTM) of the study area with 20m resolution was derived from the EPMAPS cartographic database. The INIGEMM (Instituto Nacional Geológico Minero Metalúrgico del Ecuador) provided and processed the ASTER (Advanced Spaceborne Thermal Emission and Reflection Radiometer) satellite image at 15m resolution for NDVI (Normalized Difference Vegetation Index) calculations that describe the distribution of the vegetation along the catchment. Soil information was derived from the field measurements carried out during November 2012 - January 2013, which provides soil depth and texture expressed in percentage of sand, silt and clay. The percentages of vegetation coverage and climate parameters at each elevation range are shown in Annex Table A1.

3 Materials and methods

3.1 Modelling strategy

BIOME-BGC is a biogeochemical and eco-physiological model (version 4.2 [34, 35]) that uses daily meteorological data and general stand soil information (Figure 2) to simulate the energy, carbon, nitrogen and water cycles. BIOME-BGC requires standard meteorological data as the main drivers for the ecosystem activity [39] namely maximum and minimum temperature, precipitation, incoming shortwave radiation, vapour pressure deficit. The last two parameters were generated by using the mountain climate simulator MT-CLIMB version 4.3 [36, 35] that estimate the near surface parameters based on nearby observations of temperature and precipitation. The model uses 34 parameters within the main categories for the plant functional type [43] and it was applied independently for each of the growth forms (as separate simulations) along the altitudinal gradient for 10 years of simulation (2000–2009).

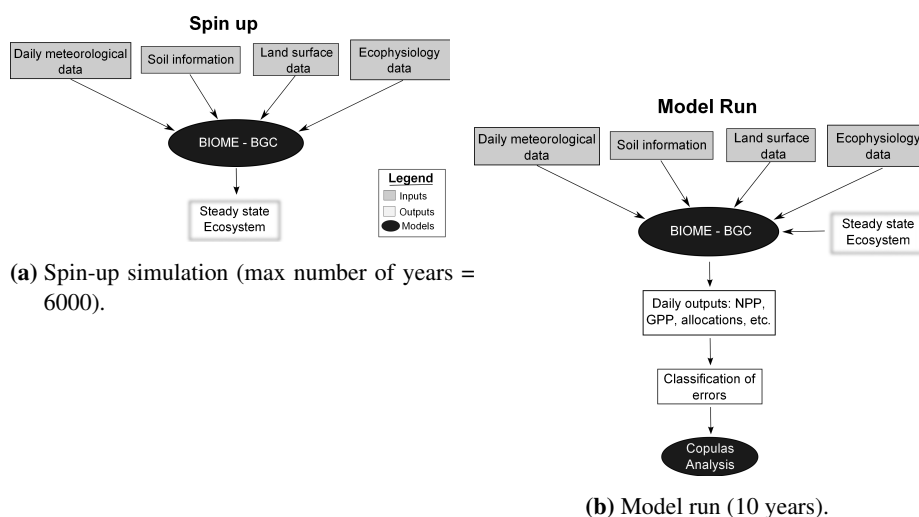


Figure 2: Simplified scheme of the modelling and analysis steps followed to obtain the classification of errors starting from the input data.

The first step of the model was to perform a spin-up running to get the model into equilibrium [37] and estimate the steady state of the system, typically 3000–4800 yr (Figure 2) through the 10-year daily driver record. The spin-up runs simulate a hypothetical steady state for primary production in a preindustrial condition. The optimized GPP parameters are responsive to soil nutrient status, CO₂ atmospheric concentration and the rate of nitrogen deposition, which in

turn have effects on soil organic matter and plant biomass states. Further inner processes can be found in detailed in the research done by [34].

3.2 Simulation of GPP

BIOME-BGC simulates gross primary production (GPP), which is based on the Farquhar photosynthesis model [Farquhar et al.(1980)] that takes into account photosynthetically active radiation, atmospheric carbon dioxide concentration, air temperature, vapour pressure deficit, precipitation, atmospheric nitrogen deposition, leaf area index and available nitrogen content in soil. Photosynthesis is also driven by indirect controls that operate through the influence of environmental conditions on the mineralization of nitrogen due to litter and soil organic matter decomposition [29]. The GPP represents the total amount of CO₂ that is fixed by the plants through photosynthesis and it has proved to be a good indicator of ecosystem's health. For instance the spatial variability of GPP ranges from 2400 gC/m²/yr in tropical evergreen forests to less than 30 gC/m²/yr in temperate deserts [15]. The GPP was estimated for each growth form at three different altitudes to check individual CO₂ assimilation. One-way analysis of variance (ANOVA) was applied to test the differences of growth forms of vegetation and altitudinal ranges in the GPP.

3.3 Error analysis of GPP

We call error (Err) to the absolute difference of GPP of the dominant vegetation (tussocks) in an averaged elevation from now on GPP_{REF} , and the near real situation of having a vegetation heterogeneity clustered in three growth forms at each altitudinal range from now on GPP_R ,

$$Err_R(t) = GPP_{REF}(t) - GPP_R(t) \quad (1)$$

where, R is the altitudinal range (4100 m, 4300 m, 4500 m), and t the time. The near real GPP that is taking place in each altitudinal range (R) was calculated considering the percentage of coverage of each plant as follows:

$$GPP_R(t) = \sum_{GF} (GPP_{GF} * \%cov_{GF}). \quad (2)$$

The GF is the growth form vegetation represented by tussock TU , acaulescent rosette AR and cushion CU . The $\%cov$ is the percentage of coverage. The errors at each altitudinal range (Err_R) were classified based on four quantiles (q) as follows: Class 1 when $Err_R < q_{(1)}$, Class 2 when $q_{(1)} \leq Err_R < q_{(2)}$, Class 3 when $q_{(2)} \leq Err_R < q_{(3)}$, and Class 4 when $Err_R \geq q_{(3)}$.

3.4 Copula analysis and classification

Copula was first introduced by [33], the theorem was mainly used in the theory of probabilistic metric spaces, then it was used to incorporate the information on the dependence structure between two or more random variables. Basically [33] showed a bivariate joint distribution H with margins $F(x)$ and $G(y)$ related with a copula function C , then

$$H(x, y) = C(F(x), G(y)). \tag{3}$$

Out of the several families of copulas functions for statistical modelling, the ones presented below were selected as the most widely used (Table 1) [41]. Figure 3 shows the main steps used to test the copulas functions and based on the maximum pseudo-likelihood select which family to use that fit the data. All tests were conducted using R [26], using the copula package [14]. We performed a classification based on groups of the same probability for the transformed data of GPP against SWR and VPD, respectively.

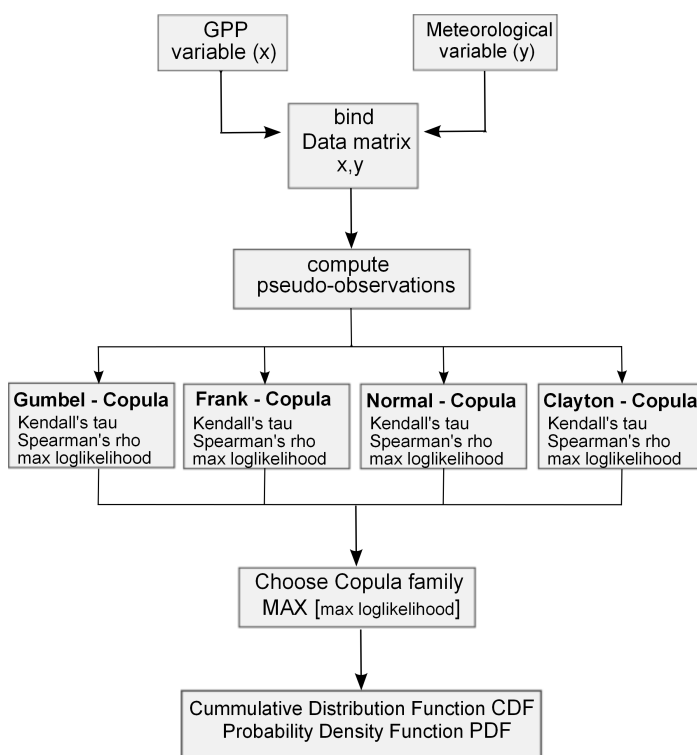


Figure 3: Flow chart scheme of the procedure of copulas family selection.

<i>Copula family</i>	<i>Function</i> $C(\mu_1, \mu_2)$	θ – domain
<i>Gumbel</i>	$\mu_1 \mu_2 (1 + \theta(1 - \mu_1)(1 - \mu_2))$	$-1 \leq \theta \leq +1$
<i>Frank</i>	$-\frac{1}{9} \log \left(1 + \frac{(e^{-\theta\mu_1} - 1)(e^{-\theta\mu_2} - 1)}{e^{-\theta} - 1} \right)$	$\theta \in (-\infty, \infty)$
<i>Normal</i>	$\phi_G[\phi^{-1}(\mu_1), \phi^{-1}(\mu_2); \theta]$	$-1 \leq \theta \leq +1$
<i>Clayton</i>	$(\mu_1^{-\theta} + \mu_2^{-\theta} - 1)^{-1/\theta}$	$\theta \in (0, \infty)$

Table 1: Copula functions families and the range of parameter Φ .

4 Results and discussion

4.1 Daily estimation of GPP

The BIOME-BGC simulated the GPP variation along an altitudinal gradient for each growth form. The GPP decreases from lower to higher altitudes (ANOVA $F = 1387.02$, $df=2$, $p < 0.001$) (Figure 4, panel a) and also differ from one growth form to another (ANOVA $F = 2246.38$, $df=2$, $p < 0.001$), being the tussock (TU) the one with higher GPP (Figure 4, panel b). On average, results from the simulation of the GPP are high for low elevations (0.44 ± 0.17 gC/m²/day) and low for higher elevations (0.35 ± 0.13 gC/m²/day). We can attribute significant GPP variation along an altitudinal gradient since elevations are characterized by the climatology. In addition, the meteorological variables indirectly control the decomposition rates of organic matter and litter, which differs from plant to plant. These decomposition rates and soil characteristics restrict the mineralization of nitrogen, which in turn influences in the GPP estimations. Low GPP is associated to slow nutrient cycling due to low rates of decomposition of cold soils (annual mean temperature of R3 is 4.82 ± 0.37 °C). Figure 4, panels c & d show a two-way interaction plot to depict the main effects of two independent variables and their interaction. The analysis revealed similar information as above, where the altitudinal ranges (R1, R2, R3) have a main effect on the GPP for the three growth forms of vegetation (TU, AR, CU) and vice versa. The mean value of GPP in TU shows higher and significant values in comparison to the AR and CU along the altitudinal gradient.

The mean values of GPP for AR and CU are within the same range and it shows interaction in higher elevations. The stratification of the ecosystem in three altitudinal ranges shows differences in individual contributions to the overall GPP of the basin. We cannot attribute the GPP variations to the model input

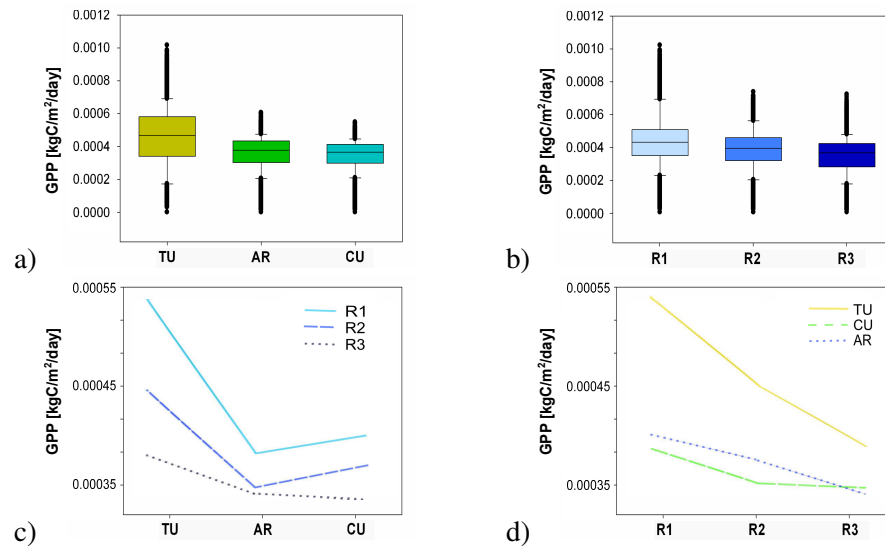


Figure 4: Boxplots (95% confidence interval) showing the GPP variation in (a) Growth forms of vegetation and (b) altitudinal ranges. Interaction plots of (c) growth form and (d) altitudinal ranges.

data only. The catchment, as part of the Andean highlands, is a very heterogeneous landscape and moisture conditions as a result of localized precipitation and soil features diverge at different locations.

4.2 GPP response to meteorology

The model behaviour in terms of daily and interannual fluctuations suggests the sensitivity to the meteorological conditions. The sensitivity of GPP is difficult to attribute to a single meteorological variable since most of them are dependent of each other [17]. However, we consider it crucial to investigate the strength and relationship between each meteorological variable and GPP variability for future trends in climate variation. Figure 5 shows the GPP model simulations and the daily meteorological variables at 4100 masl for 10 years period simulation. It shows the sensitivity of TU along the simulation and its large amplitude and frequency (<standard deviation) in comparison to the other growth forms. We calculate Spearman's rho correlation coefficient to check possible relationships between GPP and meteorological variables on a monthly basis. For all three growth forms of vegetation in the low and mid elevations, the GPP is positively correlated to SWR ($\rho > 0.52$, $p < 0.05$) to VPD ($\rho > 0.65$, $p < 0.01$), mean and maximum temperature ($\rho > 0.60$, $p < 0.05$ and $\rho > 0.64$, $p < 0.01$)

respectively). Conversely, for higher elevations no good association between variables was found showing a total independence of variables. The GPP is more responsive to SWR, VPD and temperature as the main components for photosynthesis to produce chemical energy.

4.3 Order of errors

Table 2 summarizes the comparison between the reference GPP_{REF} and the near real GPP_R of each altitudinal range. There is an overestimation of GPP for all cases and it increases towards higher elevations. The most noticeable difference is visible in the higher altitudinal range, where the use of a reference value leads to an overestimation of more than 30%. The total overestimation in 10 years is 5038.57 [tonC] if the entire study basin is accounted for this overestimation. This value represents 24.1% more than what it has already been produced from 2000 to 2009. These results not only imply that there are substantial inefficiencies in the GPP calculation in the Andean grasslands due to generalized parameterizations but the implications in climate trends of concluding that the ecosystem is fixing more CO_2 than it actually does.

Setup	Area	GPP	Difference	Difference	10-year dif-
	[km^2]	[$kgC/m^2/day$]	from refer- ence	from ref- erence	ference from reference
			[$kgC/m^2/day$]	%	[TonC]
R1	3.04	0.463	0.056	10.85	625.30
R2	4.16	0.395	0.131	24.85	1984.15
R3	5.34	0.240	0.125	34.15	2429.12

Table 2: Gross primary production (GPP) of LCH basin at three altitudinal ranges (including all three growth forms of vegetation) in comparison to reference (Tussock as the main growth form at an averaged elevation) (2000 - 2009 Mean).

After we classified the error classes based on their quantiles for each altitudinal range, we can see in Figure 6 (panel a) that the difference between the GPP_{REF} and GPP_R is low. This means that the errors produced by taking GPP_{REF} instead of GPP_R could be accepted if we consider that the range of errors could be negligible if those lie up to $q_{(2)}$. In the same figure in panel b) errors increase for most of the years except for 2005 and 2006, where we assume these could be related to climate drivers that make this difference imperceptible. These errors expand even more in higher elevations (Figure 6 panel c); however

it could be seen a homogeneity in their amplitudes along the time series. Different behaviours can be seen when comparing the GPP with the climatic drivers SWR and VPD in the three altitudinal ranges (Figure 7). At altitudinal range 1 (R1), the variation in GPP between 0.1×10^{-3} and 0.5×10^{-3} can be of both error class 1 and 2 (Figure 7 panel a&d). Events of GPP higher than 0.6×10^{-3} are not related to the variation of the climate variables. An overlap of error classes 1, 2 and 3 could be seen for altitudinal range 2 (R2) (Figure 7 panel b&e), suggesting a need for another dimension (variable) that could identify what characterizes this range of variation. For altitudinal range 3 (R3) there is a complete overlap of all error classes that implies large errors throughout the GPP (Figure 7 panel c&f). It can be seen a concentration of these large errors when GPP is between 0.5 and 1.5 indicating a higher deviation between the mean and the region.

4.4 Copula-based models

Table 3 summarizes the copula family chosen for separate simulations of GPP of plant vegetation and altitudinal ranges. The maximum likelihood is not always generated from the same copula family, however it can be noticed that the prevailing copulas for the comparison between GPP and the meteorological variables are Frank and Normal. These type of copulas are widely applied due to their strength to emphasize the correlation among large losses defined by the tails of the distributions. We also applied this approach in the combined GPP for each altitudinal range and the maximum likelihood function favors the Frank copula, which stood out from the rest for all bivariate distributions. As a matter of exercise we only show the results from the altitudinal range R2 against the two main climate drivers SWR and VPD. Figure 8 panel a & b shows a clear correlation of the extreme tails but not elsewhere in the distribution. A Frank copula matches these aspects of the data in the probability density function (PDF) panel c & d and the cumulative distribution function (CDF) fitted our data suggesting a well chosen copula family (panel e & f). The copulas have demonstrated to be a powerful tool and it helps to easily identify areas of GPP vs climate drivers that can be translated to probabilities of sensitive and unresponsive biological production. The point color on the CDF indicates groups of the same range of probability of the combination GPP-SWR (panel g) and GPP-VPD (panel h). The red color indicates that the probability of having that association of GPP vs the meteorological drivers is very high.

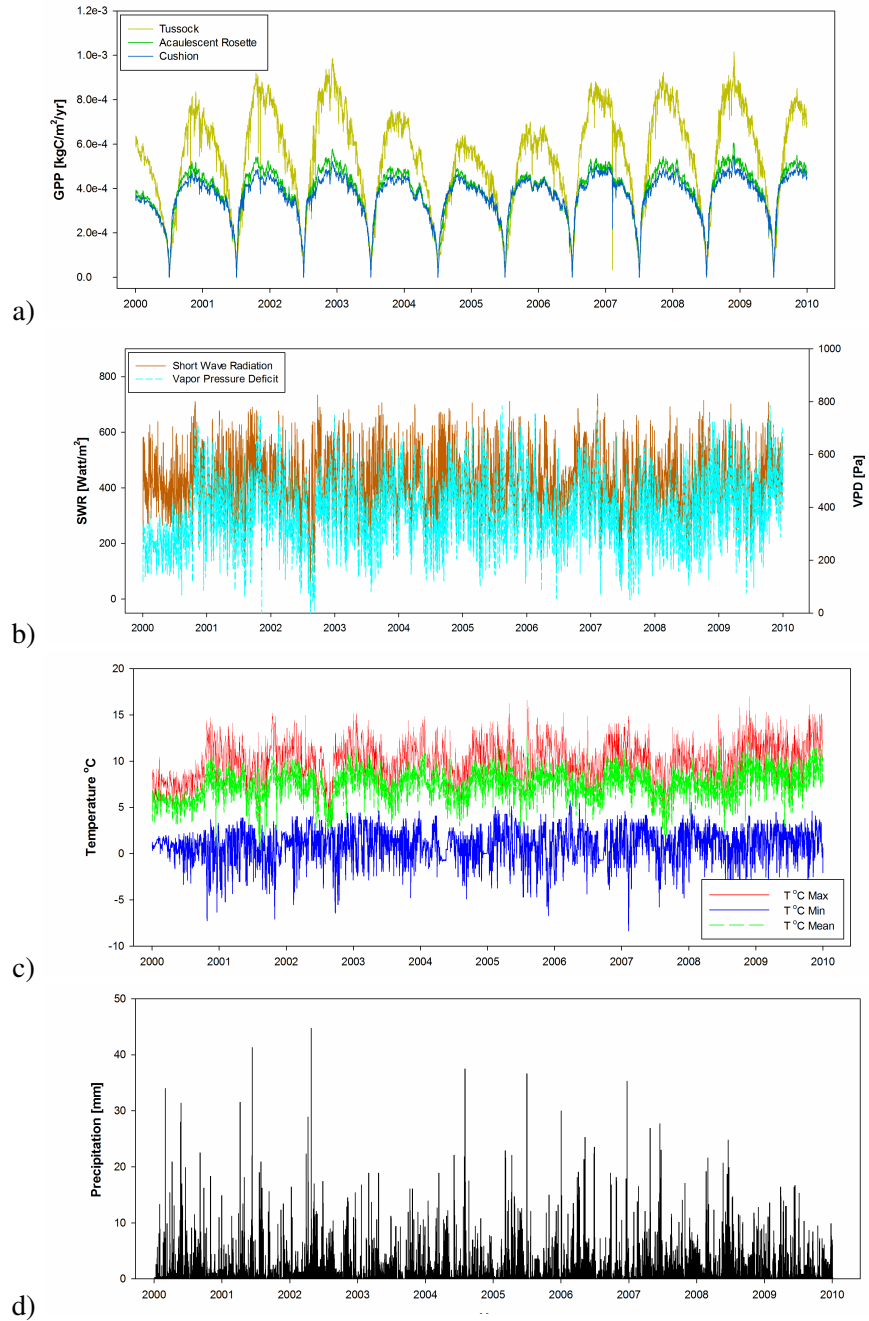


Figure 5: GPP and meteorological daily variations at elevation R1 (4000-4200 masl) in 10 years (2000 - 2010). (a), Daily outputs of GPP for three growth forms of vegetation (b), Short wave radiation (SWR) and vapour pressure deficit (VPD) (c), Temperature max, min and mean; and (d), precipitation.

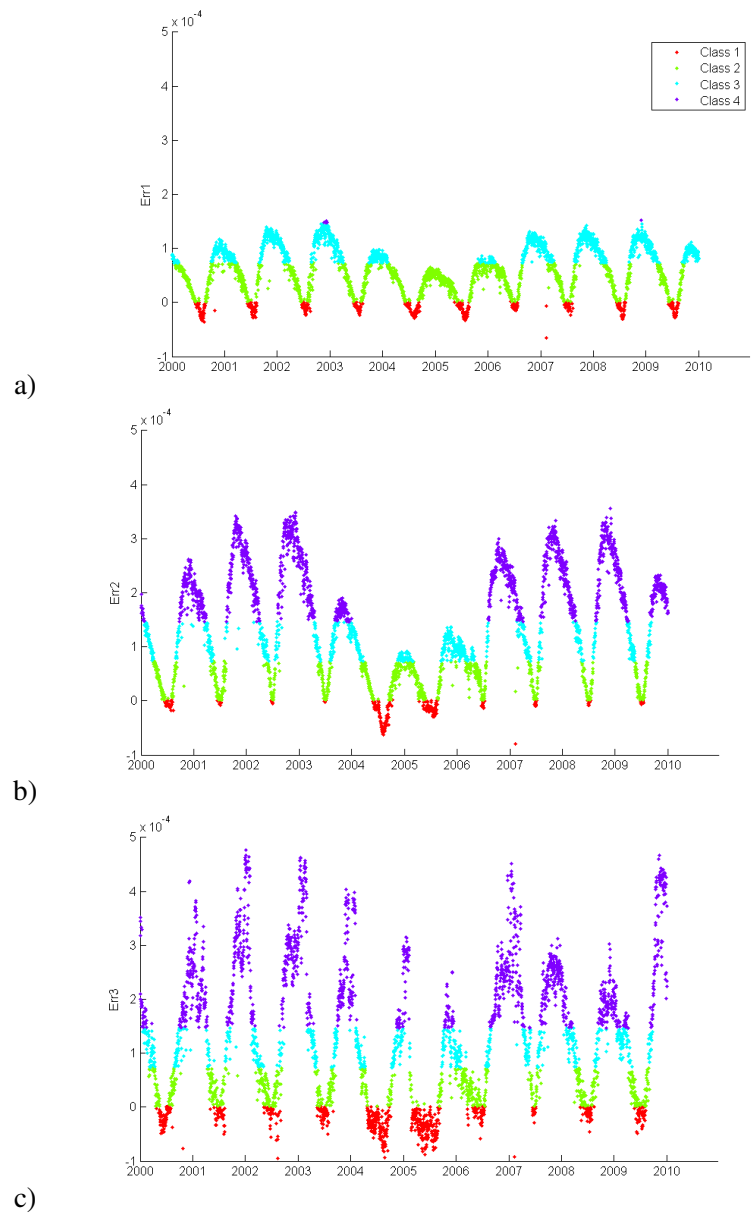


Figure 6: Error classification based on quartiles for three altitudinal ranges: (a) R1(4000-4200 masl), (b) R2(4200-4400 masl), and (c) R3(4400-4600 masl).

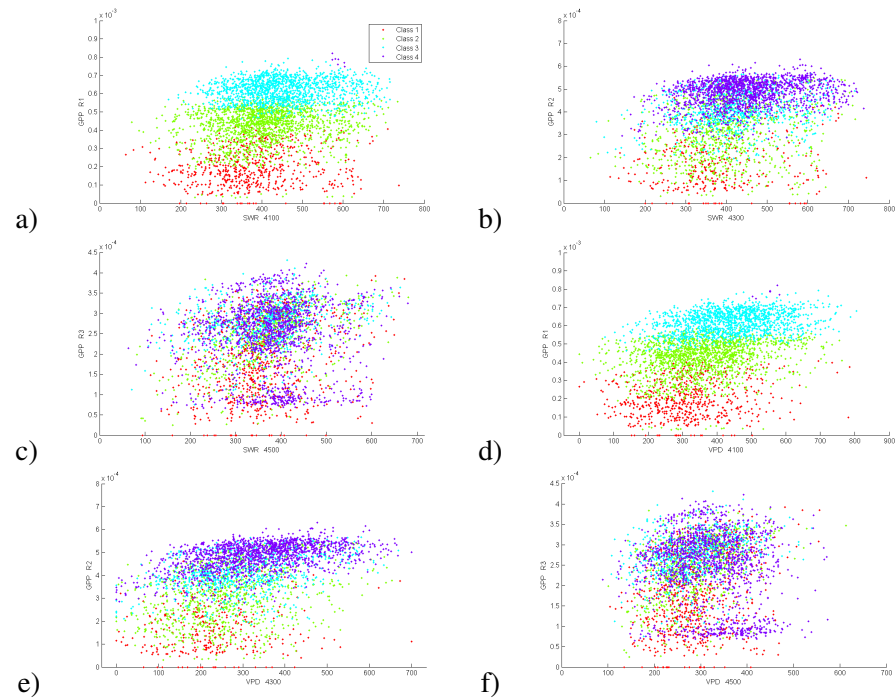


Figure 7: GPP vs meteorological variables: short wave radiation (SWR) and vapour pressure deficit (VPD). The classification is based on quartiles at R1: panels a, d), at R2: panels b, e), and at R3: panels c, f).

GPP	SWR	VPD	PRE	TEMP	Tmax	Tmin
TU_R1	Frank	Frank	Gumbel	Normal	Frank	Normal(n.s.)
AR_R2	Frank	Frank	Gumbel	Normal	Frank	Frank(n.s.)
CU_R3	Frank(n.s.)	Normal(n.s.)	Normal(n.s.)	Normal(n.s.)	Normal(n.s.)	Frank(n.s.)
TU_R1	Frank	Normal	Frank	Normal	Normal	Frank(n.s.)
AR_R2	Frank	Frank	Frank	Normal	Normal	Frank(n.s.)
CU_R3	Clayton	Clayton	Clayton(n.s.)	Clayton	Clayton	Clayton(n.s.)
TU_R1	Clayton	Normal	Normal	Normal	Normal	Clayton(n.s.)
AR_R2	Frank	Frank	Frank	Normal	Normal	Frank(n.s.)
CU_R3	Clayton	Clayton	Clayton(n.s.)	Clayton	Clayton	Clayton(n.s.)

n.s. = not significant

Table 3: Copula family chosen for individual simulation that combines each growth form of vegetation and altitudinal ranges.

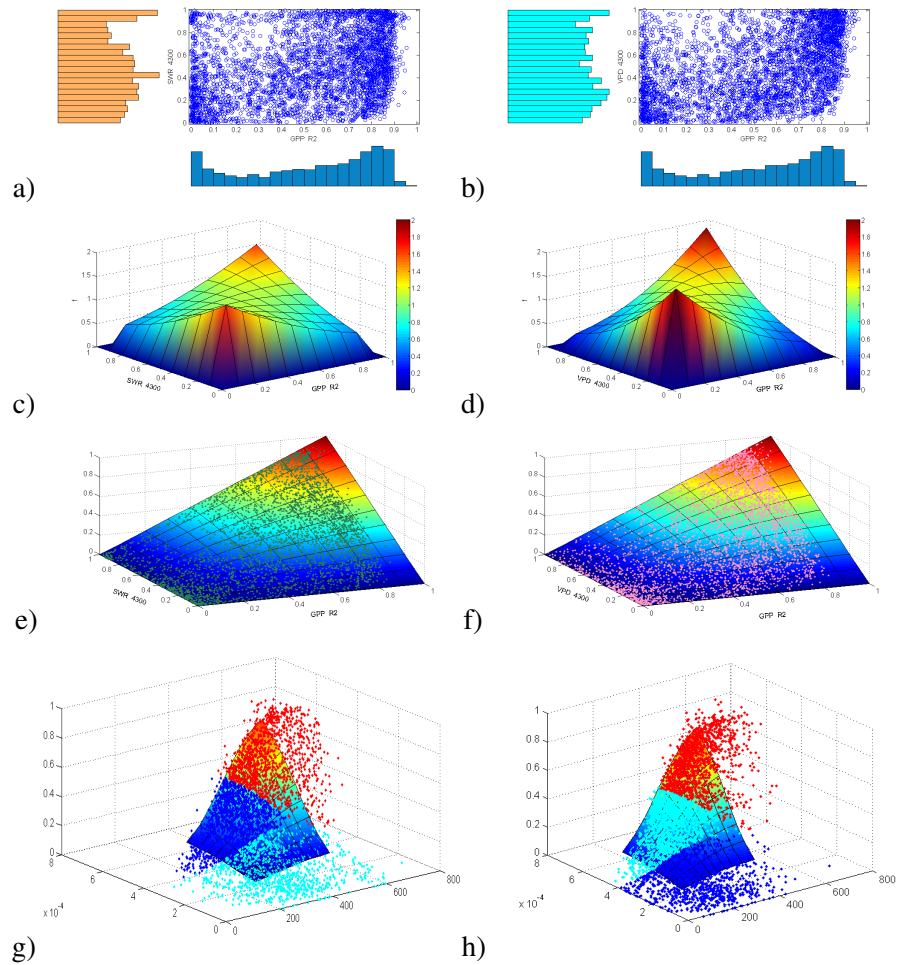


Figure 8: Analysis of GPP vs SWR and VPD in altitudinal range R2. Scatter plots of transformed data: panels a, b. Probability density function (PDF) of Frank Copulas: panels c, d. Cumulative density function (CDF) that fit the data: panels e, f. Clustering of groups with the same probability: panels: g,h.

5 Conclusions

In this paper a methodology to analyze the difference between carbon flux simulations based on averaged eco-physiological parameters (dominant vegetation and mean elevation) with altitude and growth forms of vegetation variations has been developed. In this Andean grassland region parameters in a landscape vegetation were heterogeneous and this effort has been neglected in the past due to manifold constraints but it is necessary to identify GPP deviations along environmental and ecophysiological gradients to better represent the terrestrial carbon assimilation by Andean grasslands. We found a clear overestimation of 24% in average caused by the use of generalized parameters for this region. The large variation in GPP suggests a relationship of a joint effect of radiation and VPD, which are non-linear responses due to the interaction with nitrogen dynamics in the model. However, the copulas bivariate analysis helped, at least partly, to classify expected responses of GPP in dependence with a specific range of these climatic drivers. The overall scope of this work will include a hydrological study since plant production is limited by water availability. Microclimates are driven by the ENSO phenomena which can determine a variation of GPP during dry seasons.

Acknowledgment

Financial support came from SENESCYT (Secretaría Nacional de Educación Superior, Ciencia, Tecnología e Innovación) and from the Dutch Ministry of Foreign Affairs (DUPC program at UNESCO-IHE). Other institutions that also cooperated in the provision of key information and data are EPMAPS, EPN, INAMHI, IRD, INIGEMM, Ministry of Environment, Herbario Nacional del Ecuador. The opinions expressed herein are those of the author(s) and do not necessarily reflect views of any of the Institutions named above. Our thanks also go to Adriana Guatame, Santiago Oña, Franz Betancourt and Washington Lomas.

References

- [1] Bell, S. (1999) "A beginner's guide to uncertainty of measurement", *Measurement Good Practice Guide* 11(2), National Physical Laboratory, Teddington, United Kingdom.
- [2] Cavieres, L.A.; Quiroz, C.L.; Molina-Montenegro, M.A.; Muñoz, A.A.; Pauchard, A. (2005) "Nurse effect of the native cushion plant *Azorella mo-*

nantha on the invasive non-native *Taraxacum officinale* in the high-Andes of central Chile”, *Perspectives in Plant Ecology, Evolution and Systematics* **7**: 217–226.

- [3] Chowdhary, H.; Singh, V.P. (2010) “Reducing uncertainty in estimates of frequency distribution parameters using composite likelihood approach and copula-based bivariate distributions”, *Water Resources Research* **46**: 1–23.
- [4] Cleveland, C.C.; Townsend, A.R.; Schimel, D.S.; Fisher, H.; Howarth, R.W.; Hedin, L.O.; Perakis, S.S.; Latty, E.F.; Von Fischer, J.C.; Elseroad, A.; Wasson, M.F. (1999) “Global patterns of terrestrial biological nitrogen (N₂) fixation in natural ecosystems”, *Global Biogeochemical Cycles* **13**: 623–645.
- [5] Cong, R.G.; Brady, M. (2012) “The interdependence between rainfall and temperature: Copula analyses”, *The Scientific World Journal* **2012**: 1–12.
- [6] Crabtree, R.; Potter, C.; Mullena, R.; Sheldona, J.; Huang, S.; Harm-sena, J.; Rodmanc, A.; Jeanc, C. (2009) “A modeling and spatio-temporal analysis framework for monitoring environmental change using NPP as an ecosystem indicator”, *Remote Sensing of Environment* **113**: 1486–1496.
- [7] Diemer, M. (1998) “Leaf lifespans of high-elevation, a seasonal Andean shrub species in relation to leaf traits and leaf habit”, *Global Ecological Biogeography* **7**: 457–465.
- [8] Dufour, A.; Gadallah, F.; Wagner, H.H.; Guisan, A.; Buttler, A. (2006) “Plant species richness and environmental heterogeneity in a mountain landscape: effects of variability and spatial configuration”, *Ecography* **29**: 573–584.
- [9] FAO (2010) “Grassland carbon sequestration: management, policy and economics”, *Proceedings of the Workshop on the Role of Grassland Carbon Sequestration in the Mitigation of Climate Change*, Food and Agriculture Organization of the United Nations, Rome.
- [Farquhar et al.(1980)] Farquhar, G.D.; von Caemmerer, S.; Berry, J.A. (1980) “A biogeochemical model of photosynthetic CO₂ assimilation in leaves of C3 species”, *Planta* **149**: 78–90.
- [10] Gebremichael, M.; Krajewski, W.F. (2007) “Application of copulas to modeling Ttemporal sampling errors in satellite-derived rainfall estimates”, *Journal of Hydrologic Engineering* **12**: 404–408.

- [11] Genest, C.; Favre, A.C. (2007) "Everything you always wanted to know about copula modeling but were afraid to ask", *Journal of Hydrologic Engineering* **12**: 347–368.
- [12] Gill, R.A.; Jackson, R.B. (2000) "Global patterns of root turnover for terrestrial ecosystems", *New Phytologist* **147**: 13–31.
- [13] Gräler, B.; Kazianka, H.; Espindola, G.M. de (2010) "Copulas, a novel approach to model spatial and spatio-temporal dependence", *GIScience for Environmental Change Symposium Proceedings* **40**: 49–54.
- [14] Hofert, M.; Kojadinovic, I.; Maechler, M.; Yan, J. (2013) "Multivariate dependence with copula", in: Repository CRAN.
- [15] Ito, A.; Oikawa, T. (2004) "Global mapping of terrestrial primary productivity and Light use efficiency with a process-based model", in: M. Shiyomi et al. (Eds.) *Global Environmental Change in the Ocean and on Land*: 343–358.
- [16] Jung, M.; Le Maire, G.; Zaehle, S.; Luysaert, S.; Vetter, M.; Churkina, G.; Ciais, P.; Viovy, N.; Reichstein, M. (2007a) "Assessing the ability of three land ecosystem models to simulate gross carbon uptake of forests from boreal to Mediterranean climate in Europe", *Biogeosciences* **4**: 647–656.
- [17] Jung, M.; Vetter, M.; Herold, M.; Churkina, G.; Reichstein, M.; Zaehle, S.; Ciais, P.; Viovy, N.; Bondeau, A.; Chen, Y.; Trusilova, K.; Feser, F.; Heimann, M. (2007b) "Uncertainties of modeling gross primary productivity over Europe: A systematic study on the effects of using different drivers and terrestrial biosphere models", *Global Biogeochemical Cycles* **21**(4): 1–12.
- [18] Kelliher, F.M.; Leuning, R.; Raupach, M.R.; Schulze, E.D. (1995) "Maximum conductances for evaporation from global vegetation types", *Agriculture for Meteorology* **73**: 1–16.
- [19] Kimball, J.S.; Running, S.W.; Saatchi, S.S. (1999) "Sensitivity of boreal forest regional water flux and net primary production simulations to sub-grid-scale land cover complexity", *Geophysical Research* **104**(D22): 789–801.
- [20] Kimball, J.S.; Keyser, A.R.; Running, S.W.; Saatchi, S.S. (2000) "Regional assessment of boreal forest productivity using an ecological process model and remote sensing parameter maps", *Tree Physiology* **20**: 761–775.

- [21] Line, M.A.; Loutit, M.W. (1973) “Studies on non-symbiotic nitrogen fixation in New Zealand tussock-grassland soils”, *New Zealand Journal of Agricultural Research* **16**: 87–94.
- [22] Minaya, V.; Corzo, G.; Romero-Saltos, H.; van der Kwast, J.; Lantinga, E.; Galarraga-Sanchez, R.; Mynett, A.E. (In press) “Altitudinal analysis of carbon stocks and biomass distribution in the páramo”.
- [23] Myneni, R.B.; Keeling, C.D.; Tucker, C.J.; Asrar, G.; Nemani, R.R. (1997) “Increased plant growth in the northern high latitudes between 1981-1991”, *Nature* **386**: 698–702.
- [24] Nobel, P.S. (1991) *Physicochemical and Environmental Plant Physiology*. Academic Press, San Diego.
- [25] Phoenix, G.K.; Hicks, W.K.; Cinderby, S.; Kuylenstierna, J.C.I.; Stock, W.D.; Dentener, F.J.; Giller, K.E.; Austin, A.T.; Lefroy, R.D.B.; Gimeno, B.S.; Ashmore, M.R.; Ineson, P. (2006) “Atmospheric nitrogen deposition in world biodiversity hotspots: The need for a greater global perspective in assessing N deposition impacts”, *Global Change Biology* **12**: 470–476.
- [26] R Development Core Team (2007) “A Language and Environment for Statistical Computing”, in: <http://www.R-project.org/>.
- [27] Ralph, C.P. (1978) “Observations on *Azorella Compacta (Umbelliferae)*, a tropical Andean cushion plant”, *Biotropica* **10**(1): 62–67.
- [28] Ramsay, P.M.; Oxley, E.R.B. (1997) “The growth form composition of plant communities in the ecuadorian páramos”, *Plant Ecology* **131**: 173–192.
- [29] Running, S.W.; Thornton, P.E.; Nemani, R.; Glassy, J.M. (Eds) (2000) *Global terrestrial gross and net primary productivity from the Earth Observing System*. Springer-Verlag, New York.
- [30] Scott, D. (1961) “Methods of measuring growth in short tussocks”, *New Zealand Journal of Agricultural Research* **4**(3-4): 282–285.
- [31] Shaver, G.R.; Canadell, J.; Chapin, F.S.; Gurevitch, J.; Harte, J.; Henry, G.; Ineson, P.; Jonasson, S.; Melillo, J.; Pitelka, L.; Rustad, L. (2000) “Global warming and terrestrial ecosystems: a conceptual framework for analysis”, *BioScience* **50**(10): 871–882.

- [32] Sitch, S.; Smith, B.; Prentice, I.C.; Arneth, A.; Bondeau, A.; Cramer, W.; Kaplan, J.O.; Levis, S.; Lucht, W.; Sykes, M.T.; Thonicke, K.; Venevsky, S. (2003) "Evaluation of ecosystem dynamics, plant geography and terrestrial carbon cycling in the LPJ dynamic global vegetation model", *Global Change Biology* **9**(2): 161–185.
- [33] Sklar, A. (1959) *Fonctions de Répartition à n Dimensions et Leurs Marges*. Publications de l'Institut de Statistique de l'Université de Paris.
- [34] Thornton, P.E. (1998) *Regional Ecosystem simulation: combining surface and satellite based observations to study linkages between terrestrial energy and mass budgets*. Ph.D. Thesis, University of Montana, Missoula.
- [35] Thornton, P.E. (2000) "Simultaneous estimation of daily solar radiation and humidity from observed temperature and precipitation: an application over complex terrain in Austria", *Agricultural and Forest Meteorology* **104**: 255–271.
- [36] Thornton, P.E.; Running, S.W. (1999) "An improved algorithm for estimating incident daily solar radiation from measurements of temperature, humidity, and precipitation", *Agricultural and Forest Meteorology* **93**: 211–228.
- [37] Thornton, P.E.; Rosenbloom, N.A. (2005) "Ecosystem model spin-up: Estimating steady state conditions in a coupled terrestrial carbon and nitrogen cycle model", *Ecological Modelling* **89**: 25–48.
- [38] Trusilova, K.; Churkina, G. (2008) *The terrestrial ecosystem model GBIOME-BGCv1*. Max-Planck Institut für Biogeochemie, Jena, Germany.
- [39] Trusilova, K.; Trembath, J.; Churkina, G. (2009) "Parameter estimation and validation of the terrestrial ecosystem model BIOME-BGC using eddy-covariance flux measurements", Technical Report 16, Max Planck Institut für Biogeochemie, Jena, Germany.
- [40] VEMAP (1995) "Vegetation/ecosystem modeling and analysis project: comparing biogeography and biogeochemistry models in a continental scale study of terrestrial ecosystem responses to climate change and CO₂ doubling", *Global Biogeochemical Cycles* **9**: 407–437.
- [41] Wang, M.; Rennolls, K.; Tang, S. (2008) "Bivariate distribution modeling of tree diameters and heights: dependency modeling using copulas", *Forest Science* **54**: 284–293.

- [42] Wang, W.; Ichiic, K.; Hashimoto, H.; Michaelisa, A.R.; Thornton, P.E.; Lawe, B.E.; Nemanib, R.R. (2009) “A hierarchical analysis of terrestrial ecosystem model Biome-BGC: Equilibrium analysis and model calibration”, *Ecological Modelling* **220**: 2009–2023.
- [43] White, M.A.; Thornton, P.E.; Running, S.W.; Nemani, R.R. (2000) “Parameterization and sensitivity analysis of the BIOME-BGC terrestrial ecosystem model: Net primary production controls”, *Earth Interactions* **4**(3): 1–85.
- [44] Wullschleger, S.D. (1993) “Biochemical limitations to carbon assimilation in C3 plants - A retrospective analysis of the A/Ci curves from 109 species”, *Journal of Experimental Botany* **44**: 907–920.
- [45] Yan, J. (2006) *Multivariate Modeling with Copulas and Engineering Applications*, in: H. Pham (Ed.) *Handbook in Engineering Statistics*:. 973–990.
- [46] Zhao, M.; Running, S.W.; Nemani, R.R. (2006) “Sensitivity of Moderate Resolution Imaging Spectroradiometer (MODIS) terrestrial primary production to the accuracy of meteorological reanalyses”, *Geophysical Research* **111**: 1–13.

Annex A

Parameter	R1	R2	R3	Reference
<i>Site and soil</i>				
Elevation (m)	4100	4300	4500	-
Site latitude (°)		-0.4665		-
Albedo (DIM)	0.1723	0.1759	0.1753	-
Effective soil depth (m)	1.7	1	.5	[22]
Sand:silt:clay ratio	19:66:15	24:59:17	58:20:22	[22]
Nitrogen deposition ($\text{kgNm}^{-2}\text{year}^{-1}$)		0.000389		[25]
Nitrogen fixation ($\text{kgNm}^{-2}\text{year}^{-1}$)		0.0003		[21] [4]
<i>Meteorological data</i>				
Mean annual air temperature (°C)	7.31±1.44	6.53±0.35	4.82±0.37	-
Mean annual precipitation (mm)	925.1±100.8	1337.4± 196.0	1176.2±184.7	-
<i>Vegetation</i>				
% coverage TU	59.65	56.61	45.38	-
% coverage AR	28.79	36.89	20.61	-
% coverage CU	7.03	3.2	1.1	-
% coverage rock	4.53	3.29	32.91	-

Table A1: Meteorological data summarize the climate file (annual means \pm SD) based on 10 years of daily data (2000-2009). Where no reference is given, the value given was obtained from different sources (see text). Altitudinal ranges are R1: 4000-4200 masl; R2: 4200-4400 masl; R3: 4400-4600 masl.

Parameter	TU	AR	CU	Reference
<i>Turnover and mortality parameters</i>				
Annual leaf & fine root turnover	1.84±0.18	1.44±0.35	1.13±0.16	[7]
Annual whole plant mortality		0.25±0.08		[12]
Current growth proportion	0.02±0.01	0.06±0.00	0.000128	TU:[30] AR:[7] CU:[27]
<i>Allocation parameters</i>				
Fine root C: leaf C	0.54±0.10	0.68±0.02	0.88±0.06	[22]
<i>Carbon to nitrogen parameters</i>				
C:N of leaves	76.19±11.39	26.04±2.48	24.36±2.16	[22]
C:N of leaf litter	121.17±18.12	41.41±3.95	38.74±3.43	[22]
C:N roots	25.01±1.40	28.52±4.29	30.58±7.95	[22]
<i>Labile, cellulose, and lignin parameters</i>				
Litter labile	0.51±0.01	0.51±0.04	0.42±0.02	[22]
Litter cellulose	0.28±0.02	0.17±0.05	0.22±0.05	[22]
Litter lignin	0.21±0.03	0.32±0.07	0.36±0.06	[22]
Root labile	0.52±0.06	0.54±0.02	0.54±0.05	[22]
Root cellulose	0.20±0.05	0.17±0.06	0.19±0.06	[22]
Root lignin	0.28±0.08	0.29±0.03	0.27±0.03	[22]
<i>Canopy parameters</i>				
Water interception ($LAI^{-1}day^{-1}$)		0.0225		[43]
Light extinction		0.48		[43]
SLA (projected area basis) ($m^2kg^{-1}C$)	15.08±5.85	11.80±0.84	13.82±1.62	[43]
Shaded/sunlit SLA		2.0		[43]
All-sided: projected leaf area		2.0		[43]
Leaf N in Rubisco (%)	2.20±0.70	0.34±0.03	0.37±0.07	[44]
Maximum g_s ($mm s^{-1}$)	0.011	0.02	0.0217	TU: [18] AR & CU: [2]
Cuticular conductance ($mm s^{-1}$)	0.00011	0.0002	0.00022	TU: [18] AR & CU: [2]
Boundary layer conductance ($mm s^{-1}$)	0.022	0.04	0.03	[24]
ψ_L start of g_s reduction (MPa)		-0.73		[43]
ψ_L complete of g_s reduction (MPa)		-2.7		[43]
VPD start of g_s reduction (Pa)	1000			[43]
VPD complete of g_s reduction (Pa)	5000			[43]

Table A2: Simulation ecophysiological parameters by growth form (TU: tussock, AR: acaulescent rosettes, CU: cushion). Abbreviations: C= carbon; N= nitrogen; LAI: leaf area index; SLA= specific leaf area; g_s = stomatal conductance; ψ_L = leaf water potential; and VPD= vapour pressure deficit.